

Momentum Dependence of Resonant Inelastic X-Ray Scattering Spectrum in Insulating Cuprates

K. Tsutsui, T. Tohyama, and S. Maekawa

Institute for Materials Research, Tohoku University, Sendai 980-8577, Japan

(Received 26 May 1999)

The resonant inelastic x-ray scattering spectrum in insulating cuprates is examined by using the exact diagonalization technique on small clusters in the two-dimensional Hubbard model with second and third neighbor hopping terms. When the incident photon energy is tuned near the Cu K absorption edges, we find that the features of the unoccupied upper Hubbard band can be extracted from the spectrum through an anisotropic momentum dependence. They provide an opportunity for the understanding of the different behavior of hole- and electron-doped superconductors.

PACS numbers: 74.25.Jb, 71.10.Fd, 78.70.Ck

Resonant inelastic x-ray scattering (RIXS) is developing very rapidly into a powerful technique to investigate elementary excitations in the strongly correlated electron systems [1–5]. The application of this technique to insulating copper oxides has made it possible to observe an excitation due to a local charge transfer between copper and oxygen [3] and local d - d excitations on copper site [4]. In addition, it has been demonstrated that, by using high resolution experiments [5], the momentum-dependent measurement of the charge-transfer gap is possible when the incident photon energy ω_i is tuned through a Cu K absorption edge. Thus, the RIXS can be a useful probe to obtain information on the momentum dependence of the elementary excitations.

One of the elementary excitations in the insulating cuprates is the charge-transfer process from the occupied Zhang-Rice singlet band (ZRB) [6] composed of Cu $3d_{x^2-y^2}$ and O $2p_\sigma$ orbitals to the unoccupied upper Hubbard band (UHB). The dispersion of ZRB has been extensively studied by angle-resolved photoemission spectroscopy (ARPES) experiments on the parent compounds of high T_c superconductors [7–9]: A d -wave-like dispersion was observed along the $(0, \pi)$ - $(\pi, 0)$ line with the minimum of the binding energy at $(\pi/2, \pi/2)$ [9]. On the contrary, the dispersion relation and spectral properties of the unoccupied UHB have not been examined and thus remain to be understood. The information of UHB is of crucial importance for the understanding of the motion of electrons in the electron-doped superconductors. In addition, it may be useful to know if the particle-hole symmetry is required for the high temperature superconductivity.

In this Letter, we examine the RIXS spectrum for the Cu K edge, and demonstrate that the characteristic features of the dispersion of UHB can be extracted from the momentum dependence of the spectrum. To see this, we use the half-filled single-band Hubbard model to describe the occupied ZRB and unoccupied UHB by mapping ZRB onto the lower Hubbard band (LHB) in the model. Then, we incorporate Cu $1s$ and $4p$ orbitals into the model to include the $1s$ -core hole and excited $4p$ electron into the intermediate state of the RIXS process. The long-range hoppings

are also introduced in the Hubbard model with realistic values obtained from the analysis of ARPES data. We find a characteristic momentum dependence of the Cu K -edge RIXS spectrum: The energy of the threshold of the RIXS spectrum at $(\pi/2, \pi/2)$ is higher than that at $(0, 0)$, whereas the energy of the threshold at $(\pi/2, 0)$ is lower than that at $(0, 0)$. This anisotropic dependence is explained by the dispersion of the UHB which has the minimum energy at $(\pi, 0)$ due to the long-range hoppings. The determination of the UHB will contribute to the understanding of the different behavior of hole- and electron-doped superconductors [8,10].

We map the ZRB onto the LHB, which is equivalent to the elimination of O $2p$ orbitals. Such mapping was used in the analysis of O $1s$ x-ray absorption spectrum [11]. The Hubbard Hamiltonian with second and third neighbor hoppings for the $3d$ electron system is written as

$$H_{3d} = -t \sum_{\langle \mathbf{i}, \mathbf{j} \rangle_{1st}, \sigma} d_{\mathbf{i}, \sigma}^\dagger d_{\mathbf{j}, \sigma} - t' \sum_{\langle \mathbf{i}, \mathbf{j} \rangle_{2nd}, \sigma} d_{\mathbf{i}, \sigma}^\dagger d_{\mathbf{j}, \sigma} - t'' \sum_{\langle \mathbf{i}, \mathbf{j} \rangle_{3rd}, \sigma} d_{\mathbf{i}, \sigma}^\dagger d_{\mathbf{j}, \sigma} + \text{H.c.} + U \sum_{\mathbf{i}} n_{\mathbf{i}, \uparrow}^d n_{\mathbf{i}, \downarrow}^d, \quad (1)$$

where $d_{\mathbf{i}, \sigma}^\dagger$ is the creation operator of a $3d$ electron with spin σ at site \mathbf{i} , $n_{\mathbf{i}, \sigma}^d = d_{\mathbf{i}, \sigma}^\dagger d_{\mathbf{i}, \sigma}$, the summations $\langle \mathbf{i}, \mathbf{j} \rangle_{1st}$, $\langle \mathbf{i}, \mathbf{j} \rangle_{2nd}$, and $\langle \mathbf{i}, \mathbf{j} \rangle_{3rd}$ run over the first, second, and third nearest-neighbor pairs, respectively, and the rest of the notation is standard.

Figure 1 shows the schematic process of Cu K -edge RIXS. An absorption of an incident photon with energy ω_i , momentum \mathbf{K}_i , and polarization $\boldsymbol{\epsilon}_i$ brings about the dipole transition of an electron from Cu $1s$ to $4p$ orbital [process (a) in Fig. 1]. In the intermediate states, $3d$ electrons interact with a $1s$ -core hole and a photoexcited $4p$ electron via the Coulomb interactions so that the excitations in the $3d$ electron system are evolved [process (b)]. The $4p$ electron goes back to the $1s$ orbital again and a photon with energy ω_f , momentum \mathbf{K}_f , and polarization $\boldsymbol{\epsilon}_f$ is emitted [process (c)]. The differences of the energies and the momenta between incident and emitted photons are transferred to the $3d$ electron system.

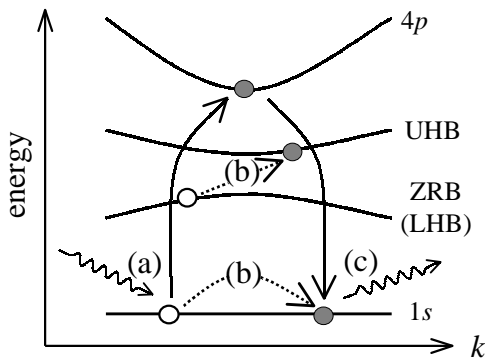


FIG. 1. Schematic picture of the Cu K -edge RIXS process. An incident photon is absorbed, and dipole transition $1s \rightarrow 4p$ is brought about [process (a)], and through the intermediate state [process (b)], the photoexcited $4p$ electron goes to $1s$ again and a photon is emitted [process (c)].

In the intermediate state, there are a $1s$ -core hole and a $4p$ electron, with which $3d$ electrons interact. Since the $1s$ -core hole is localized because of a small radius of the Cu $1s$ orbital, the attractive interaction between the $1s$ -core hole and $3d$ electrons is very strong. The interaction

is written as

$$H_{1s-3d} = -V \sum_{i,\sigma,\sigma'} n_{i,\sigma}^d n_{i,\sigma'}^s, \quad (2)$$

where $n_{i,\sigma}^s$ is the number operator of a $1s$ -core hole with spin σ at site i , and V is taken to be positive. However, since the $4p$ electron is delocalized, the repulsive interaction between the $4p$ and $3d$ electrons, as well as the attractive one between the $4p$ electron and the $1s$ -core hole, is small as compared with the $1s$ - $3d$ interaction. In addition, when the core hole is screened by the $3d$ electrons through the strong $1s$ - $3d$ interaction, an effective charge that acts on the $4p$ electron at the core-hole site becomes small. Therefore, the interactions related to the $4p$ electron are neglected for simplicity. Furthermore, we assume that the photoexcited $4p$ electron enters into the bottom of the $4p_z$ band with momentum \mathbf{k}_0 , where the z axis is perpendicular to the CuO_2 plane. This assumption is justified as long as the Coulomb interactions associated with the $4p$ electron are neglected and the resonance condition is set to the threshold of the $1s \rightarrow 4p_z$ absorption spectrum [12]. Under these assumptions, the RIXS spectrum is expressed as

$$I(\Delta\mathbf{K}, \Delta\omega) = \sum_{\alpha} \left| \langle \alpha | \sum_{\sigma} s_{\mathbf{k}_0 - \mathbf{K}_f, \sigma} p_{\mathbf{k}_0, \sigma} \frac{1}{H - E_0 - \omega_i - i\Gamma} p_{\mathbf{k}_0, \sigma}^{\dagger} s_{\mathbf{k}_0 - \mathbf{K}_i, \sigma}^{\dagger} | 0 \rangle \right|^2 \delta(\Delta\omega - E_{\alpha} + E_0), \quad (3)$$

where $H = H_{3d} + H_{1s-3d} + H_{1s,4p}$, $H_{1s,4p}$ being kinetic and on-site energy terms for a $1s$ -core hole and a $4p$ electron, $\Delta\mathbf{K} = \mathbf{K}_i - \mathbf{K}_f$, $\Delta\omega = \omega_i - \omega_f$, $s_{\mathbf{k},\sigma}^{\dagger}$ ($p_{\mathbf{k},\sigma}^{\dagger}$) is the creation operator of the $1s$ -core hole ($4p$ electron) with momentum \mathbf{k} and spin σ , $|0\rangle$ is the ground state of the half-filled system with energy E_0 , $|\alpha\rangle$ is the final state of the RIXS process with energy E_{α} , and Γ is the inverse of the relaxation time in the intermediate state. In Eq. (3), the terms $H_{1s,4p}$ are replaced by ε_{1s-4p} which is the energy difference between the $1s$ level and the bottom of the $4p_z$ band.

The RIXS spectrum of Eq. (3) is calculated on $(\sqrt{8} \times \sqrt{8})$, $(\sqrt{10} \times \sqrt{10})$, and (4×4) -site clusters with a periodic boundary condition by using a modified version of the conjugate-gradient method together with the Lanczös technique. We will show the results for the (4×4) -site cluster in the following.

The values of the parameters are as follows: $t'/t = -0.34$, $t''/t = 0.23$, $U/t = 10$, $V/t = 15$, and $\Gamma/t = 1$ with $t = 0.35$ eV. The values of t , t' , and t'' are the same as those used in the analysis of ARPES data of the high T_c superconductors based on the t - t' - t'' - J model [8,13]. The value of U is obtained from the relations $J = 4t^2/U$ and $J/t = 0.4$. The value of V is set to be larger than that of U . The results shown below are insensitive to the magnitude of V as well as of Γ [14].

Before going into the RIXS spectrum, we mention the resonance condition in RIXS. To determine the condition, we have to examine the Cu $1s$ x-ray absorption

spectroscopy (XAS) spectrum defined as

$$D(\omega) = \frac{1}{\pi} \text{Im} \langle 0 | s_{\mathbf{k}_0 - \mathbf{K}_i, \sigma} p_{\mathbf{k}_0, \sigma} \frac{1}{H - E_0 - \omega - i\Gamma_{\text{XAS}}} p_{\mathbf{k}_0, \sigma}^{\dagger} s_{\mathbf{k}_0 - \mathbf{K}_i, \sigma}^{\dagger} | 0 \rangle, \quad (4)$$

where H is the same as that in Eq. (3). It is necessary to tune the incident photon energy ω_i to the energy region where the Cu $1s$ XAS spectrum appears. The inset in Fig. 2 shows $D(\omega)$, where a two-peak structure appears, i.e., the broad one at about $\omega - \varepsilon_{1s-4p} = -20t$ and the sharp one at about $-13t$. The former mainly contains configurations that the core-hole site is doubly occupied by the $3d$ electrons ($U - 2V = -20t$), while the latter dominantly contains configurations that the core-hole site is singly occupied ($-V = -15t$). This means that, when the incident energy is tuned around the former structure, the information about UHB can be extracted from the RIXS spectrum. Thus, we set ω_i to the threshold of the XAS spectrum denoted by the arrow in the inset.

Figure 2 shows the momentum dependence of the RIXS spectrum. The spectra below $\Delta\omega/t \sim 2$ and above $\Delta\omega/t \sim 5$ have different origins: The former comes from the excitations related to the spin degree of freedom such as two-magnon Raman scattering, the energy scale of which is so small that the spectrum is hard to observe [5]. On the other hand, the latter is related to the excitations from LHB to UHB. The vertical dotted line in the figure denotes the position of the low-energy

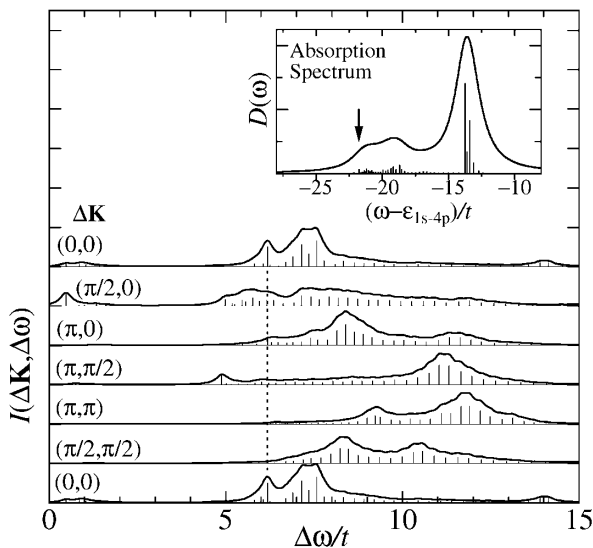


FIG. 2. Resonant inelastic x-ray scattering spectra for Cu K -edge in a half-filled Hubbard model with long-range hoppings. The spectra of the elastic scattering process at $\Delta\mathbf{K} = (0,0)$ are not shown. The parameters used are $U/t = 10$, $V/t = 15$, $\Gamma/t = 1$, $t'/t = -0.34$, and $t''/t = 0.23$. The vertical dotted line denotes the position of the peak at $\Delta\mathbf{K} = (0,0)$ for guide to eyes. The δ functions (the vertical thin solid lines) are convoluted with a Lorentzian broadening of $0.2t$. The inset shows the Cu $1s$ absorption spectrum with $\Gamma_{\text{XAS}}/t = \Gamma/t = 1.0$, and the incident photon energy ω_i is set to the value denoted by the arrow.

peak at $\Delta\mathbf{K} = (0,0)$ for guide to the eyes. The spectra strongly depend on the momentum showing a feature that the weight shifts to a higher-energy region with increasing $|\Delta\mathbf{K}|$. This momentum dependence is also obtained in the 10-site cluster calculations. In addition, the threshold of the spectrum at $\Delta\mathbf{K} = (\pi/2,0)$ and $(\pi,\pi/2)$ is lower in energy than that at $(0,0)$. At $\Delta\mathbf{K} = (\pi/2,\pi/2)$, however, the spectrum appears above the threshold at $(0,0)$, resulting in an anisotropic momentum dependence between the spectra along $(0,0)$ to $(\pi/2,0)$ and along $(0,0)$ to $(\pi/2,\pi/2)$. We note that such an anisotropic feature cannot be observed in the RIXS spectrum of the Hubbard model without t' and t'' (not shown) [15]. In the 8-site cluster the spectrum at $\Delta\mathbf{K} = (\pi/2,\pi/2)$ is lower in energy than that at $(\pi,0)$, which is consistent with the above feature.

In the intermediate state, the excitations of the $3d$ electrons from the occupied to unoccupied states are caused by the interaction with the $1s$ -core hole, i.e., $H_{1s-3d} = -V/N \sum_{\mathbf{k}_1 \sim \mathbf{k}_4, \sigma, \sigma'} \delta_{\mathbf{k}_2 - \mathbf{k}_1, \mathbf{k}_3 - \mathbf{k}_4} d_{\mathbf{k}_1, \sigma}^\dagger d_{\mathbf{k}_2, \sigma} s_{\mathbf{k}_3, \sigma'}^\dagger s_{\mathbf{k}_4, \sigma'}$. The operator $d_{\mathbf{k}_1, \sigma}^\dagger d_{\mathbf{k}_2, \sigma}$ represents a particle-hole excitation. Therefore, we analyze the RIXS process by decomposing into such a particle-hole excitation in order to understand the anisotropic momentum dependence of the threshold along $(0,0)$ to $(\pi/2,0)$ and along $(0,0)$ to $(\pi/2,\pi/2)$ in Fig. 2.

As a first step, we consider the particle-hole excitation as the convolution of the single-particle excitation

spectra $A(\mathbf{k}, \omega)$ between occupied LHB and unoccupied UHB. Figure 3 shows $A(\mathbf{k}, \omega)$ in the half-filled Hubbard model with t' and t'' terms [16]. Below the chemical potential denoted by the dotted line, a sharp peak appears at $(\pi/2, \pi/2)$ with the lowest-binding energy. In contrast, the spectrum at $(\pi, 0)$ is very broad and deep in energy. These features are consistent with the ARPES data for $\text{Sr}_2\text{CuO}_2\text{Cl}_2$ [7,8]. Above the chemical potential, the dispersion of UHB has the minimum of the energy at $\mathbf{k} = (\pi, 0)$ [17]. We show below that the $(\pi, 0)$ spectrum in UHB plays a crucial role in the RIXS spectrum with $\Delta\mathbf{K} = (\pi/2, 0)$.

Now, we examine the lowest-energy excitations with $\Delta\mathbf{K} = (0,0)$, $(\pi/2,0)$, and $(\pi/2,\pi/2)$ in the convoluted spectrum $\int_{\mathcal{E} \leq \mu} d\mathcal{E} A(\mathbf{k} + \Delta\mathbf{K}, \mathcal{E} + \omega) A(\mathbf{k}, \mathcal{E})$, where μ is the chemical potential. For the case that $\Delta\mathbf{K} = (0,0)$, the minimum excitation energy in the convoluted spectrum is $\sim 5t$ at $\mathbf{k} = (\pi, 0)$. In the same way, the lowest-energy excitation with $\Delta\mathbf{K} = (\pi/2, 0)$ in the convoluted spectrum is that from $\mathbf{k} = (\pi/2, 0)$ of LHB to $(\pi, 0)$ of UHB with the energy of $\sim 4t$. This value is smaller than that for the $\Delta\mathbf{K} = (0,0)$ case, being consistent with the relation of the thresholds of the RIXS spectra between $\Delta\mathbf{K} = (0,0)$ and $(\pi/2, 0)$. In contrast, the lowest-energy excitation with $\Delta\mathbf{K} = (\pi/2, \pi/2)$ in the convoluted spectrum is inconsistent with that in the RIXS spectrum, because the excitation energy, which is determined by the peaks at $\mathbf{k} = (\pi/2, -\pi/2)$ of LHB and at $(\pi, 0)$ of UHB, is almost the same as that for $\Delta\mathbf{K} = (\pi/2, 0)$. This means that the argument based on the convoluted spectrum of $A(\mathbf{k}, \omega)$ is insufficient to understand the anisotropic behavior of the threshold, and thus we need to treat the process of the particle-hole excitation exactly. Therefore, we introduce the spectral function $B(\mathbf{k}, \Delta\mathbf{K}; \omega)$ of the two-body Green's function, which can describe the particle-hole excitation, defined as

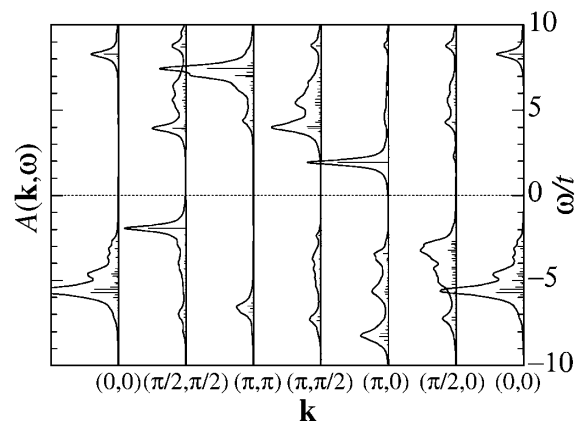


FIG. 3. Single particle excitation spectrum $A(\mathbf{k}, \omega)$ in the half-filled Hubbard model with t' and t'' terms. $t'/t = -0.34$ and $t''/t = 0.23$. The dotted line denotes the chemical potential. The δ functions are convoluted with a Lorentzian broadening of $0.2t$.

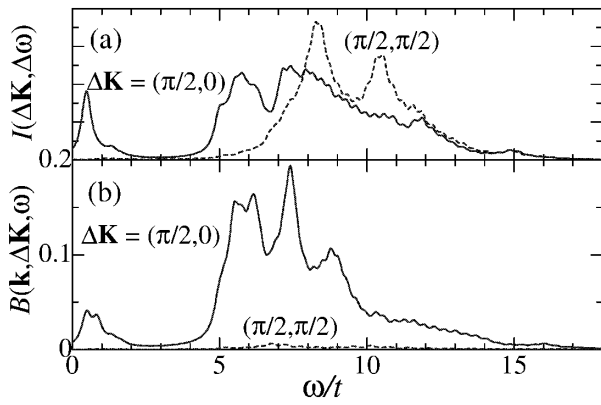


FIG. 4. Spectral function $B(\mathbf{k}, \Delta\mathbf{K}, \omega)$ which represents the particle-hole excitation process (lower panel), with $[\mathbf{k}, \Delta\mathbf{K}] = [(\pi/2, 0), (\pi/2, 0)]$ (solid line) and $[(\pi/2, -\pi/2), (\pi/2, \pi/2)]$ (dotted line). The upper panel shows the corresponding RIXS spectra $I(\Delta\mathbf{K}, \Delta\omega)$ which are given in Fig. 2.

$$B(\mathbf{k}, \Delta\mathbf{K}; \omega) = \sum_{\alpha} |\langle \alpha | \sum_{\sigma} d_{\mathbf{k}+\Delta\mathbf{K},\sigma}^{\dagger} d_{\mathbf{k},\sigma} | 0 \rangle|^2 \times \delta(\omega - E_{\alpha} + E_0), \quad (5)$$

where the states $|\alpha\rangle$ have the same point-group symmetry as that of the final states of the RIXS process. Figure 4 shows $B(\mathbf{k}, \Delta\mathbf{K}; \omega)$ with $[\mathbf{k}, \Delta\mathbf{K}] = [(\pi/2, 0), (\pi/2, 0)]$ and $[(\pi/2, -\pi/2), (\pi/2, \pi/2)]$. Note that $\mathbf{k} + \Delta\mathbf{K} = (\pi, 0)$ in both cases. The spectrum with $[\mathbf{k}, \Delta\mathbf{K}] = [(\pi/2, 0), (\pi/2, 0)]$ reproduces very well the RIXS spectrum near the threshold. The intensity of $B(\mathbf{k}, \Delta\mathbf{K}; \omega)$ with $\Delta\mathbf{K} = (\pi/2, \pi/2)$ is very small, implying that the process $\sum_{\sigma} d_{(\pi/2,0),\sigma}^{\dagger} d_{(\pi/2,-\pi/2),\sigma}$ is almost forbidden [18]. This is the origin of the small weight of $I(\Delta\mathbf{K}, \omega)$ with $\Delta\mathbf{K} = (\pi/2, \pi/2)$ around $\omega/t \sim 5$. We note that this behavior cannot be obtained by the convolution of $A(\mathbf{k}, \omega)$ mentioned above. At the higher energy region, $\omega/t \sim 7$, different processes keeping $\Delta\mathbf{K} = (\pi/2, \pi/2)$, for example, the annihilation of the $(\pi/2, 0)$ electron and the creation of the $(\pi, \pi/2)$ one, dominate the excitations. These processes induce the large weight above $\omega/t \sim 7$.

In summary, we have examined the momentum dependence of the Cu K -edge RIXS spectrum by using a numerically exact diagonalization technique on small clusters. Regarding the ZRB as the LHB, we have adopted the Hubbard model with Cu $1s$ and $4p$ bands. We have also introduced the long-range hoppings, t' and t'' , of the ZR singlet, and found that the threshold of the spectrum at $\Delta\mathbf{K} = (\pi/2, 0)$ is small compared with that at $(0, 0)$, whereas the threshold at $(\pi/2, \pi/2)$ is larger than that at $(0, 0)$. This dependence is caused by the $(\pi, 0)$ state in UHB. Thus, by examining the RIXS spectrum, we can extract the property of the unoccupied states that is crucially important for the electron-doped superconductors and also for the understanding of the behavior different from the hole-doped superconductors [8,10]. Very recently, Stanford's group reported [19] that inter-

esting data with a momentum-dependent inelastic scattering signal has been seen in the 2 eV range, which reveals the property of unoccupied states right above the charge-transfer gap. This progress in both theory and experiment will open new prospects in the physics of cuprates.

The authors thank Z.-X. Shen for valuable discussions. This work was supported by Priority-Areas Grants from the Ministry of Education, Science, Culture and Sport of Japan, CREST, and NEDO. Computations were carried out in ISSP, University of Tokyo; IMR, Tohoku University; and Tohoku University.

- [1] C.-C. Kao *et al.*, Phys. Rev. B **54**, 16 361 (1996).
- [2] S.M. Butorin *et al.*, Phys. Rev. B **55**, 4242 (1997).
- [3] J.P. Hill *et al.*, Phys. Rev. Lett. **80**, 4967 (1998).
- [4] P. Kuiper *et al.*, Phys. Rev. Lett. **80**, 5204 (1998).
- [5] P. Abbamonte *et al.*, cond-mat/9810095. The best resolution used was 0.45 eV.
- [6] F. C. Zhang and T. M. Rice, Phys. Rev. B **37**, 3759 (1988).
- [7] B. O. Wells *et al.*, Phys. Rev. Lett. **74**, 964 (1995).
- [8] C. Kim *et al.*, Phys. Rev. Lett. **80**, 4245 (1998).
- [9] F. Ronning *et al.*, Science **282**, 2067 (1998).
- [10] H. Takagi *et al.*, Physica (Amsterdam) **162C-164C**, 1001 (1989).
- [11] C. T. Chen *et al.*, Phys. Rev. Lett. **66**, 104 (1991).
- [12] The experimental data for the Cu K -edge absorption spectrum show that the out-of-plane (z) polarized peaks are lower in energy than in-plane polarized peaks [20]. In order to examine the RIXS spectrum with the single component of the $4p$ bands, we consider the case of a z -polarized photon.
- [13] In 8- and 10-site clusters, only t and t' are included for hopping parameters due to their small system sizes.
- [14] P. M. Platzman and E. D. Isaacs, Phys. Rev. B **57**, 11 107 (1998).
- [15] K. Tsutsui, T. Tohyama, and S. Maekawa (unpublished).
- [16] For $A(\mathbf{k}, \omega)$ in the Hubbard model without t' and t'' , see P. W. Leung *et al.*, Phys. Rev. B **46**, 11 779 (1992).
- [17] In the large U limit, the dispersion of the UHB is described by the single-hole dispersion of the t - t' - t'' - J model with $t < 0$, $t' > 0$, and $t'' < 0$. The sign difference comes from the fact that the carrier in UHB is an electron [see T. Tohyama and S. Maekawa, Phys. Rev. B **49**, 3596 (1994)]. Although the energy at $(\pi, 0)$ is almost the same as that at $(\pi/2, \pi/2)$ in the t - J model, the former decreases when $t'(>0)$ and $t''(<0)$ are introduced. By defining $\epsilon(\mathbf{k}) = 4t' \cos k_x \cos k_y + 2t''(\cos k_x + \cos k_y)$, the energy difference between at $(\pi/2, \pi/2)$ and $(\pi, 0)$ is proportional to $\epsilon(\pi/2, \pi/2) - \epsilon(\pi, 0) = -8t'' + 4t'$.
- [18] In the spin-density wave mean-field approximation, $B(\mathbf{k}, \Delta\mathbf{K}; \omega)$ with $[\mathbf{k}, \Delta\mathbf{K}] = [(\pi/2, -\pi/2), (\pi/2, \pi/2)]$ is rigorously zero. This is due to the effect of the coherence factor arising from the antiferromagnetic long-range order as is the case of the BCS superconductivity. The details will be shown elsewhere.
- [19] Z. Hasan, E. Isaacs, and Z.-X. Shen (unpublished).
- [20] N. Kosugi *et al.*, Chem. Phys. **135**, 149 (1989)